

Origin of the efficiency improvement in all-polymer solar cells upon annealing

M. M. Mandoc

Zernike Institute for Advanced Materials and Dutch Polymer Institute, University of Groningen, Nijenborgh 4, NL-9747 AG Groningen, The Netherlands

W. Veurman

Zernike Institute for Advanced Materials, University of Groningen, Nijenborgh 4, NL-9747 AG Groningen, The Netherlands

J. Sweelssen and M. M. Koetse

Holst Centre/TNO and Dutch Polymer Institute, P.O. Box 8550, 5605 KN Eindhoven, The Netherlands

P. W. M. Blom^{a)}

Zernike Institute for Advanced Materials, University of Groningen, Nijenborgh 4, NL-9747 AG Groningen, The Netherlands

(Received 12 July 2007; accepted 25 July 2007; published online 16 August 2007)

The origin of the enhanced efficiency upon annealing in solar cells based on blends of poly[2-methoxy-5-(3',7'-dimethyloctyloxy)-1,4-phenylene vinylene] and poly{9,9-dioctylfluorene-2,7-diyl-alt-1,4-bis[2-(5-thienyl)-1-cyanovinyl]-2-methoxy-5-(3,7-dimethyl-octyloxy)benzene} is investigated. Current-voltage measurements on solar cells and single-carrier diodes reveal that the electron and hole transport is not improved for thermally treated devices. From the analysis of the photocurrent, the authors show that the dissociation efficiency of the bound electron-hole pairs increases upon annealing, due to an increase of the initial electron-hole separation distance. © 2007 American Institute of Physics. [DOI: 10.1063/1.2772185]

Organic solar cells are promising candidates for clean energy and, compared to their inorganic counterparts, have the advantages of flexibility and low production costs. Until now, efficiencies reaching more than 4% have been obtained for slowly dried blends of regioregular poly(3-hexylthiophene) and [6,6]-phenyl C₆₁-butyric acid methyl ester (PCBM).¹⁻³ However, as most of the light is absorbed only in the polymeric phase of the blend, a promising system for organic solar cells would be a blend made of two absorbing conjugated polymers. However, with blends of poly[2-methoxy-5-(3',7'-dimethyloctyloxy)-1,4-phenylene vinylene] (MDMO-PPV) and poly[oxa-1,4-phenylene-(1-cyano-1,2-vinylene)-(2-methoxy-5-(3',7'-dimethyloctyloxy)-1,4-phenylene)-1,2-(2-cyanovinylene)-1,4-phenylene] (PCNEPV), a fill factor lower than 25% has been obtained for standard devices, while the optimized cells had an efficiency of only 0.75%.⁴ Better performing solar cells have been obtained by blending PPV derivatives with either an alternating copolymer poly{9,9-dioctylfluorene-2,7-diyl-alt-1,4-bis[2-(5-thienyl)-1-cyanovinyl]-2-methoxy-5-(3,7-dimethyl-octyloxy)benzene} (PF1CVTP) as electron acceptor⁵ or cyano substituted copolymers,⁶ with efficiency values for optimized devices reaching 1.5% and 1.7%, respectively. In both cases, an important step toward optimizing the devices is a thermal treatment. In a recent study by Yin *et al.* with cyano substituted copolymers, it has been demonstrated that upon annealing the exciplex emission of these polymer blends is strongly reduced, in combination with an increase of the photocurrent.⁷ This indicates that the photovoltaic performance is hindered by the generation of free charge carriers.⁷ In this letter, we investigate the origin

of the increased performance for MDMO-PPV:PF1CVTP solar cells upon annealing by using a recently device model for polymer based solar cells.⁸ Analysis of the charge transport and photocurrent before and after annealing shows that the dissociation efficiency of the geminate electron-hole pairs is strongly enhanced.

The devices have been prepared on indium tin oxide coated glass, on which poly(3,4-ethylenedioxythiophene):poly(4-styrene sulphonate) has been first spin coated from an aqueous solution. Subsequently, the polymer blend (1:1 weight ratio) has been spin coated from a chlorobenzene solution and, as a top electrode, 1 nm of lithium fluoride (LiF) followed by 100 nm of aluminum (Al) have been deposited by thermal evaporation. Annealing has been performed using a hot plate at 120 °C for 15 min, before the deposition of the top electrode. The solar cells have been illuminated with a halogen lamp, at an intensity of about 870 W/m². In Fig. 1, the typical photocurrent for standard and annealed cells is shown. The standard cells clearly have a lower fill factor and a lower photocurrent compared to the annealed devices. For the not annealed devices, efficiencies of about 0.5% have been obtained, whereas the annealed devices show an increase of the efficiency to about 1%.

As a first step, we model the photocurrent of the standard cells. For this, information about the charge transport in the cells is required. In Fig. 2(a), the hole current (measured in a hole-only diode with a Au top electrode) of a MDMO-PPV:PF1CVTP blend is shown. For comparison, also the hole current of a pristine MDMO-PPV hole-only device with equal thickness is shown.

Upon blending MDMO-PPV with PF1CVTP, there is no increase of the hole mobility, as is the case for MDMO-PPV:PCBM blends.⁹ In this respect, the blends of MDMO-PPV:PF1CVTP behave similar to the earlier studied MDMO-

^{a)}Electronic mail: p.w.m.blom@rug.nl

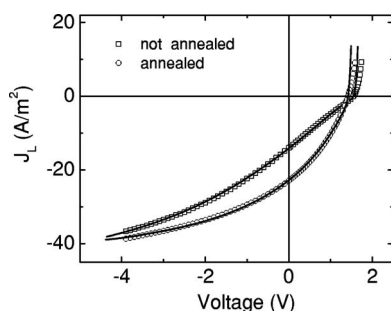


FIG. 1. Current under illumination vs voltage of a standard MDMO-PPV:PF1CVTP solar cell (squares) and of an annealed device (circles), both with an active layer thickness of about 40 nm. The solid lines are the calculated currents for the two cases, with the mobility values derived from transport measurements and the dissociation parameters: $a=0.78$ nm and $k_f=1.6 \times 10^3$ s $^{-1}$ for the standard (not annealed) device and $a=1.2$ nm and $k_f=9.5 \times 10^3$ s $^{-1}$ for the annealed device.

PPV:PCNEPV blends.¹⁰ Furthermore, to study the electron transport, electron-only diodes have been prepared on aluminum oxide bottom electrodes. As a top electrode, LiF/Al has been used. The electron current in the PF1CVTP phase in the blend shows the fingerprints of a trap-limited transport, with an exponential distribution of traps.¹¹ In Fig. 2(b), the strong thickness dependence which is characteristic for an exponential distribution of traps is shown. In the calculations, a free carrier mobility of 1×10^{-10} m 2 /V s has been used, as determined from double-carrier measurements of PF1CVTP (hole-only devices are injection limited due to the deep highest occupied molecular orbital of PF1CVTP).

Both the transport and the shape of the photocurrent of the standard MDMO-PPV:PF1CVTP cell are similar to MDMO-PPV:PCNEPV cells,¹² for which an efficiency of about 0.25% has been obtained under white light illumina-

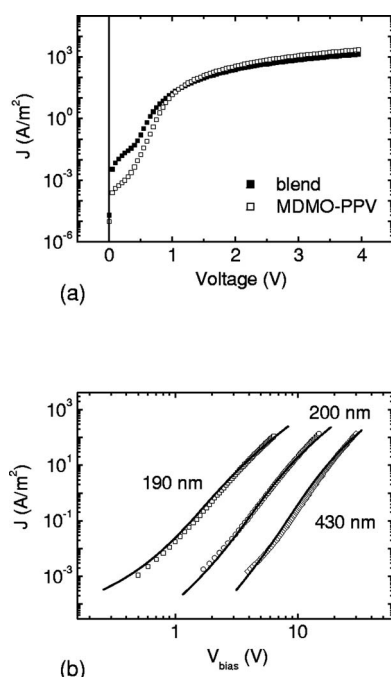


FIG. 2. (a) Hole-only current of MDMO-PPV:PF1CVTP blend (closed symbols) and of pristine MDMO-PPV (open symbols), for an active layer thickness of 55–60 nm. (b) Electron current through the PF1CVTP phase of the blend for active layers with the thickness of 190 nm (squares), 200 nm (circles), and 430 nm (diamonds). The calculated lines use an exponential trap model with $N_t=7.2 \times 10^{22}$ m $^{-3}$ and $T_t=1900$ K.

tion at 1000 W/m 2 . We have shown that the low performance of these PCNEPV based cells is due to the low carrier mobilities, low dielectric constant, and a strongly bound electron-hole (e-h) pair, all combining to an inefficient dissociation.¹² Furthermore, in these cells, a trap-controlled carrier recombination is affecting the open-circuit voltage at low light intensities.¹² Following the same approach for the standard MDMO-PPV:PF1CVTP cell, the photocurrent as a function of applied voltage can be described with the mobility values derived from transport measurements and dissociation parameters of $a=0.78$ nm and $k_f=1.6 \times 10^3$ s $^{-1}$ for the initial e-h separation distance and the decay rate of the bound e-h pair, respectively. Furthermore, a relative dielectric constant of 2.6 has been used, and trap-assisted recombination has been included using the trapping parameters, as derived from the electron transport measurements. The capture coefficient for holes to recombine with the trapped electrons is derived from the light intensity of V_{oc} and is found to be $C_p=2.0 \times 10^{-18}$ m 3 s $^{-1}$.

As shown in Fig. 1, the efficiency of the MDMO-PPV:PF1CVTP cells increases with a factor of 2 upon annealing. An important factor that can significantly contribute to this improved performance of the annealed cells is an increase of the carrier mobility as a result of the thermal treatment. In this case, not only will the charge carriers be transported faster, leading to lower recombination losses, but the dissociation efficiency of the bound e-h pairs will also be strongly enhanced.¹³ Therefore, we investigated the charge transport properties of the blends in single-carrier devices before and after annealing, as shown in Fig. 3. From the measurements on the hole-only [Fig. 3(a)] and electron-only diodes [Fig. 3(b)], it can be concluded that there is no significant increase of the charge transport properties in the blends upon annealing. Furthermore, we also verified that the dark current of the solar cells was independent on the annealing procedure, as it can be seen in Fig. 3(c). As the leakage current is unchanged after annealing, effects such as removal of pinholes can be thus ruled out.

With the transport properties of the annealed devices known, we now apply our device model to the photocurrent of the annealed devices, as shown in Fig. 1 (solid line). The model calculations demonstrate that the increase of the photocurrent and fill factor upon annealing can be mainly explained by an increase of the initial e-h separation distance a , going from $a=0.78$ nm for the standard (not annealed) device to $a=1.2$ nm for the annealed device. Furthermore, an even better fit is obtained when the decay rate of the bound pair is slightly adapted from $k_f=1.6 \times 10^3$ s $^{-1}$ to $k_f=9.5 \times 10^3$ s $^{-1}$ upon annealing. This increase of a can be attributed to a change of morphology upon annealing. Before annealing, the polymers are strongly intermixed, leading to strongly localized electrons and holes. Upon annealing, the phase separation is increased, giving rise to larger domains of both polymers. Since charge carriers are not confined by the energy offsets of the other polymer within these domains, this is expected to result in an increased delocalization of the charge carriers. A similar conclusion had been drawn by Yin *et al.* who attributed the decrease of exciplex emission after annealing to demixing of the polymer phases.⁷

In conclusion, we have shown that for MDMO-PPV:PF1CVTP solar cells, the increase in performance upon annealing is not due to an increase in the carrier mobility, but to a better dissociation process of the bound electron-hole

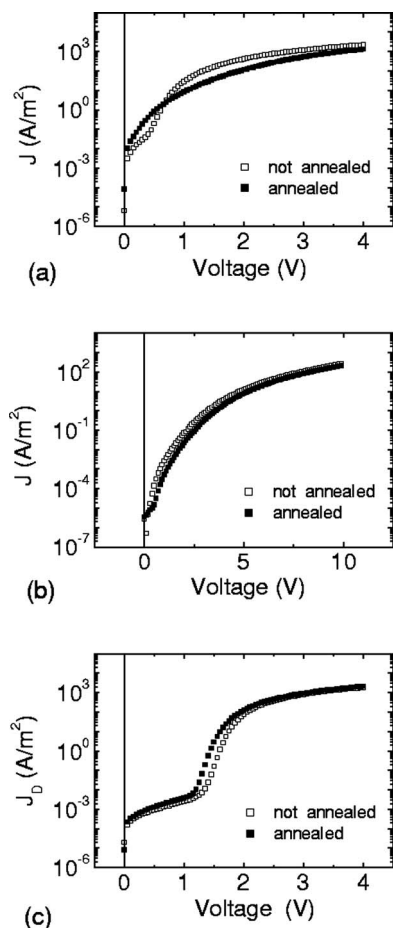


FIG. 3. (a) J - V characteristics of a hole-only device before (open symbols) and after annealing (closed symbols) for an active layer thickness of ~ 40 nm. (b) J - V characteristics of a standard (not annealed) electron-only diode (open symbols) and of an annealed device (closed symbols) with the thickness of the active layer of 220–230 nm. (c) Dark J - V characteristics of a solar cell before (open symbols) and after annealing (closed symbols), for an active layer thickness of ~ 40 nm.

pairs. Modeling of the photocurrent reveals that the electrons and holes, which are still Coulombically bound, are more spatially separated upon annealing, which facilitates the dissociation into free charge carriers. This increased delocalization is proposed to arise from a change in the morphology of the polymer blend, where after annealing, larger domains are formed. In order to further optimize all-polymer solar cells, the dissociation should be further optimized by using polymers with an increased dielectric constant and an increased charge carrier mobility.

This work forms part of the research program of the Dutch Polymer Institute (DPI), Project No. 324.

- ¹W. Ma, C. Yang, X. Gong, K. Lee, and A. J. Heeger, *Adv. Funct. Mater.* **15**, 1617 (2005).
- ²G. Li, V. Shrotriya, J. Huang, Y. Yao, T. Moriarty, K. Emery, and Y. Yang, *Nat. Mater.* **4**, 864 (2005).
- ³M. Reyes-Reyes, K. Kim, and D. L. Carroll, *Appl. Phys. Lett.* **87**, 083506 (2005).
- ⁴S. C. Veenstra, W. J. H. Verhees, J. M. Kroon, M. M. Koetse, J. Sweelssen, J. J. A. M. Bastiaansen, H. F. M. Schoo, X. Yang, A. Alexeev, J. Loos, U. S. Schubert, and M. M. Wienk, *Chem. Mater.* **16**, 2503 (2004).
- ⁵M. M. Koetse, J. Sweelssen, K. T. Hoekerd, H. F. M. Schoo, S. C. Veenstra, J. M. Kroon, X. Yang, and J. Loos, *Appl. Phys. Lett.* **88**, 083504 (2006).
- ⁶T. Kietzke, H.-H. Hörhold, and D. Neher, *Chem. Mater.* **17**, 6532 (2005).
- ⁷C. Yin, T. Kietzke, D. Neher, and H.-H. Hörhold, *Appl. Phys. Lett.* **90**, 092117 (2007).
- ⁸L. J. A. Koster, E. C. P. Smits, V. D. Mihailetschi, and P. W. M. Blom, *Phys. Rev. B* **72**, 085205 (2005).
- ⁹C. Melzer, E. J. Koop, V. D. Mihailetschi, and P. W. M. Blom, *Adv. Funct. Mater.* **14**, 865 (2004).
- ¹⁰M. M. Mandoc, W. Veurman, L. J. A. Koster, M. M. Koetse, J. Sweelssen, B. de Boer, and Paul W. M. Blom, *J. Appl. Phys.* **101**, 104512 (2007).
- ¹¹P. Mark and W. Helfrich, *J. Appl. Phys.* **33**, 205 (1962).
- ¹²M. M. Mandoc, W. Veurman, L. J. A. Koster, B. de Boer, and P. W. M. Blom, *Adv. Funct. Mater.* (to be published).
- ¹³C. L. Braun, *J. Chem. Phys.* **80**, 4157 (1984).